PLOS GENETICS

RESEARCH ARTICLE

Cyclin B3 activates the Anaphase-Promoting Complex/Cyclosome in meiosis and mitosis

Damien Garrido[1,2], **Mohammed Bourouh**[1,2,3], **Éric Bonneil**[1,4], **Pierre Thibault**[1,4], **Andrew Swan**[3]*, **Vincent Archambault**[1,2]*

1 Institute for Research in Immunology and Cancer, Université de Montréal, Montreal, Canada, **2** Département de biochimie et médecine moléculaire, Université de Montréal, Montreal, Canada, **3** Department of Biomedical Sciences, University of Windsor, Montreal, Canada, **4** Département de chimie, Université de Montréal, Montreal, Canada

* aswan@uwindsor.ca (AS); vincent.archambault.1@umontreal.ca (VA)

Citation: Garrido D, Bourouh M, Bonneil É, Thibault P, Swan A, Archambault V (2020) Cyclin B3 activates the Anaphase-Promoting Complex/Cyclosome in meiosis and mitosis. PLoS Genet 16(11): e1009184. https://doi.org/10.1371/journal.pgen.1009184

Editor: R. Scott Hawley, Stowers Institute for Medical Research, UNITED STATES

Received: July 24, 2020

Accepted: October 8, 2020

Published: November 2, 2020

Data Availability Statement: All relevant data are within the manuscript and its Supporting information files.

Funding: This work was supported by Discovery grants from the Natural Sciences & Engineering Research Council of Canada to VA and AS, and by an Operating grant from the Cancer Research Society of Canada to VA. DG was a recipient of a postdoctoral fellowship from the Fonds de Recherche du Québec – Santé (FRQS). The funders had no role in study design, data collection and

Abstract

In mitosis and meiosis, chromosome segregation is triggered by the Anaphase-Promoting Complex/Cyclosome (APC/C), a multi-subunit ubiquitin ligase that targets proteins for degradation, leading to the separation of chromatids. APC/C activation requires phosphorylation of its APC3 and APC1 subunits, which allows the APC/C to bind its co-activator Cdc20. The identity of the kinase(s) responsible for APC/C activation *in vivo* is unclear. Cyclin B3 (CycB3) is an activator of the Cyclin-Dependent Kinase 1 (Cdk1) that is required for meiotic anaphase in flies, worms and vertebrates. It has been hypothesized that CycB3-Cdk1 may be responsible for APC/C activation in meiosis but this remains to be determined. Using *Drosophila*, we found that mutations in *CycB3* genetically enhance mutations in *tws*, which encodes the B55 regulatory subunit of Protein Phosphatase 2A (PP2A) known to promote mitotic exit. Females heterozygous for *CycB3* and *tws* loss-of-function alleles lay embryos that arrest in mitotic metaphase in a maternal effect, indicating that CycB3 promotes anaphase in mitosis in addition to meiosis. This metaphase arrest is not due to the Spindle Assembly Checkpoint (SAC) because mutation of *mad2* that inactivates the SAC does not rescue the development of embryos from $CycB3^{-/+}$, $tws^{-/+}$ females. Moreover, we found that CycB3 promotes APC/C activity and anaphase in cells in culture. We show that CycB3 physically associates with the APC/C, is required for phosphorylation of APC3, and promotes APC/C association with its Cdc20 co-activators Fizzy and Cortex. Our results strongly suggest that CycB3-Cdk1 directly activates the APC/C to promote anaphase in both meiosis and mitosis.

Author summary

In both mitosis and meiosis, the initiation of chromosome segregation (anaphase) is a crucial transition that is subject to strict regulation by evolutionarily conserved enzymes. The Anaphase-Promoting Complex/Cyclosome (APC/C) is a ubiquitin ligase complex that targets key proteins for degradation to allow the separation and ensuing segregation of chromosomes. It is known that APC/C activation requires its phosphorylation on specific

analysis, decision to publish, or preparation of the manuscript.

Competing interests: The authors have declared that no competing interests exist.

subunits. However, the identity of the kinase(s) required for this activating phosphorylation in meiosis and mitosis is unclear. The Cyclin-Dependent Kinase 1 (Cdk1) in complex with its Cyclin B3 (CycB3) subunit is a candidate for this function because CycB3 is required for anaphase in female meiosis of various animal species including vertebrates. We have investigated this possibility in the fruit fly *Drosophila*. We found that CycB3-Cdk1 collaborates with Protein Phosphatase 2A—another mitotic regulator—to promote anaphase in mitosis in addition to meiosis. We also show that CycB3 interacts with the APC/C, phosphorylates the APC/C on a key subunit for its activation, and promotes the binding of the APC/C to its mitotic and meiotic Cdc20 co-activator subunits. Our results strongly suggest that CycB3-Cdk1 directly activates the APC/C to promote anaphase in meiosis and mitosis.

Introduction

Mitosis and meiosis (collectively referred to as M-phase) are distinct modes of nuclear division resulting in diploid or haploid products, respectively. In animals, both require the breakdown of the nuclear envelope, the condensation of chromosomes and their correct attachment on a microtubule-based spindle, where chromosomes are under tension and chromatids are held together by cohesins. Progression through these initial phases requires multiple phosphorylation events of various protein substrates by mitotic kinases including Cyclin-Dependent Kinases (CDKs) activated by their mitotic cyclin partners [1]. M-phase completion from this point (mitotic exit) requires the degradation of mitotic cyclins, and the dephosphorylation of several mitotic phosphoproteins by phosphatases including Protein Phosphatase 2A (PP2A) [2]. Mitotic exit begins with the segregation of chromosomes in anaphase. In mitosis, sister chromatids segregate. In meiosis I, replicated homologous chromosomes segregate, and in the subsequent meiosis II, sister chromatids segregate. Nuclear divisions are completed with the reassembly of a nuclear envelope concomitant with the decondensation of chromosomes [3]. How mitosis and meiosis are alike and differ in the molecular mechanisms of their exit programs is not completely understood.

Chromosome segregation is triggered by the Anaphase-Promoting Complex/Cyclosome (APC/C), a multi-subunit E3 ubiquitin ligase [4–7]. By catalysing the addition of ubiquitin chains on the separase inhibitor securin, the APC/C targets it for degradation by the proteasome [8,9]. As a result, separase cleaves cohesins, allowing separated chromosomes to migrate towards opposing poles of the spindle [10,11]. Activation of the APC/C in mitosis requires its recruitment of its co-factor Cdc20 [12,13]. This recruitment can be prevented by the Spindle-Assembly Checkpoint (SAC), a complex mechanism that allows the sequestration of Cdc20 until all chromosomes are correctly attached on the spindle [14]. Cdc20 binding to the APC/C is also inhibited by its phosphorylation at CDK sites [5]. Phosphatase activity is then required to dephosphorylate Cdc20 and allow its binding of the APC/C for its activation of anaphase [15–17]. In addition, phosphorylation of the APC/C itself is required to allow Cdc20 binding [18]. Phosphorylation of APC3/Cdc27 and APC1 is key to this process. Phosphorylation of APC3 at CDK sites promotes the subsequent phosphorylation of APC1, inducing a conformational change in APC1 that opens the Cdc20 binding site [19,20]. However, the precise identity of the kinase(s) involved in this process *in vivo* is unknown.

At least 3 types of cyclins contribute to M-phase in animals: Cyclins A, B and B3 [21,22]. The Cyclin A type (A1 and A2 in mammals) can activate Cdk1 or Cdk2 and is required for mitotic entry, at least in part by allowing the phosphorylation of Cdc20 to prevent its binding

and activation of the APC/C [23]. This allows mitotic cyclins to accumulate without being ubiquitinated prematurely by the APC/C and degraded. The Cyclin B type (B1 and B2 in mammals) also promotes mitotic entry and is required for mitotic progression by allowing the phosphorylation of several substrates by Cdk1 [24]. Mammalian Cyclin B3, which can associate with both Cdk1 and Cdk2, is required for meiosis but its contribution to mitosis is less clear in view of its low expression in somatic cells [25,26]. *Drosophila* possesses a single gene for each M-phase cyclin: *CycA* (*Cyclin A*), *CycB* (*Cyclin B*) and *CycB3* (*Cyclin B3*) that collaborate to ensure mitotic progression by activating Cdk1. Genetic and RNAi results suggest that they act sequentially, CycA being required before prometaphase, CycB before metaphase and CycB3 at the metaphase-anaphase transition [27,28]. CycA is the only essential cyclin, as it is required for mitotic entry [29,30]. *CycB* and *CycB3* mutants are viable, but mutations of *CycB* and *CycB3* are synthetic-lethal, suggesting redundant roles in mitosis [31]. However, mutation of *CycB* renders females sterile due to defects in ovary development, and mutant males are also sterile [31].

Drosophila CycB3 associates with Cdk1 and is required for female meiosis [31]. In *Drosophila*, eggs normally stay arrested in metaphase I of meiosis until egg laying triggers entry into anaphase I and the subsequent meiosis II. However, *CycB3* mutant eggs predominantly stay arrested in meiosis I [32]. In addition, silencing CycB3 expression in early embryos delays anaphase onset during the syncytial mitotic divisions [28]. Cyclin B3 is also required for anaphase in female meiosis of vertebrates and worms. In mice, RNAi Knock-down of Cyclin B3 in oocytes inhibits the metaphase-anaphase transition in meiosis I [33]. Recently, two groups independently knocked out the Cyclin B3-coding *Ccnb3* gene in mice and found that they were viable but female-sterile due to a highly penetrant arrest in meiotic metaphase I [34,35]. In *C. elegans*, the closest Cyclin B3 homolog, CYB-3 is required for anaphase in meiosis and mitosis [36].

How Cyclin B3 promotes anaphase in any system is unknown. One possibility is that it is required for Cdk1 to phosphorylate the APC/C on at least one of its activating subunits, APC3 or APC1. This has not been investigated. Another possibility is that inactivation of Cyclin B3 leads to an early mitotic defect that activates the SAC. This appears to be the case in *C. elegans*, because inactivation of the SAC rescues normal anaphase onset in the absence of CYB-3 [36]. However, in *Drosophila*, inactivation of the SAC by the mutation of *mad2* did not eliminate the delay in anaphase onset observed when CycB3 is silenced in syncytial embryos [28]. Similarly, in mouse oocytes, silencing Mad2 does not rescue the meiotic metaphase arrest upon Cyclin B3 depletion [33]. In other studies, SAC markers on kinetochores did not persist in metaphase-arrested *Ccnb3* KO oocytes, and SAC inactivation by chemical inhibition of Mps1 did not restore anaphase [34,35]. Finally, it is also possible that Cyclin B3 is required upstream of another event required for APC/C activation, for example the activation of a phosphatase required for Cdc20 dephosphorylation and subsequent recruitment to the APC/C.

In this study, we have investigated how CycB3 promotes anaphase in *Drosophila*. We report several lines of evidence indicating that CycB3 directly activates the APC/C in both meiosis and mitosis.

Results and discussion

CycB3 functions upstream of the APC/C and collaborates with PP2A-Tws to promote anaphase in meiosis and embryonic mitosis

In addition to the APC/C, another important enzyme for mitotic exit is PP2A-B55 [2]. We previously conducted a maternal-effect genetic screen for enhancers of mutations in *tws*, which encodes the B55 regulatory subunit of PP2A in *Drosophila*. Here, we investigated a genetic

interaction between *tws* and *CycB3*, identified in this screen. We first validated the genetic interaction using different alleles for each gene (Fig 1A). While $CycB3^{2}$ is a null allele where part of the coding sequence is deleted, $CycB3^{L6}$ ($CycB3^{L6540}$) is a hypomorphic allele induced by the insertion of a P-element [31,32]. tws^{aar1} and tws^{P} are hypomorphic alleles caused by P-element insertions [38]. We examined the phenotypes of eggs/embryos produced by mothers heterozygous for $CycB3^{2}$ and tws^{aar1} (Fig 1B). We stained for microtubules, total DNA and the pericentric DNA of the X-chromosome. Strikingly, most embryos from double-mutant mothers arrest very early in embryonic development, more specifically in metaphase of the first or second mitotic divisions. In addition, a minority of eggs arrest in metaphase of meiosis I, consistent with the known role of CycB3 in promoting anaphase in meiosis. These phenotypes are not observed in embryos from $CycB3^{2/+}$ or $tws^{aar1/+}$ mothers, where nuclear divisions proceed normally.

To test if the meiotic and mitotic metaphase arrests observed when CycB3 function is compromised are due to activation of the SAC, we introduced a null mutation in *mad2* ($mad2^{EY21687}$ = $mad2^{EY}$) known to inactivate the SAC [39]. We found that inactivation of *mad2* does not rescue the development of embryos from $CycB3^{2/+}$ $tws^{aar1/+}$ or $CycB3^{2/L6}$ mothers (Fig 1C). In fact, inactivation of *mad2* tends to enhance hatching defects when CycB3 is partially inactivated. Therefore, the metaphase arrest under a loss of CycB3 function is not caused by a defect that activates the SAC.

Based on results obtained in flies and mice, it has been suggested that CycB3 may function upstream of the APC/C to activate it [28,33–35]. We decided to test this hypothesis. First, we found that levels of CycA and CycB, both targets of the APC/C, are higher in eggs from $CycB3^{2/L6}$ mothers (Fig 1D). To test if overexpressing a stabilized form of CycB3 would conversely lead to a destabilization of mitotic cyclins, we generated transgenic flies for the expression of CycB3 mutated in its destruction box (Fig 1E) and N-terminally fused to GFP. Expression of GFP-$CycB3^{D}$ in the female germline with Gal4 results in a reduction of CycA, CycB and endogenous CycB3 levels in eggs, which do not hatch (Fig 1D). This result is consistent with an overactivation of the APC/C when CycB3 is stabilized. In this case, the prediction is that inactivation of the APC/C in this context should rescue CycB levels. This is what is observed after RNAi-silencing of APC1 or APC3, both essential subunits of the APC/C (Fig 1F and S1A Fig). Very similar results were obtained with hypomorphic mutations of *cortex* and *fizzy* (S1B Fig), the two Cdc20 co-activators of the APC/C active in female meiosis and syncytial mitoses [40–42]. These results confirm that CycB3 functions upstream of the APC/C.

Altogether, our results indicate that CycB3 promotes anaphase by acting upstream of the APC/C, not only in meiosis, but also in early embryonic mitoses, in collaboration with PP2A-Tws and independently from the SAC.

CycB3 is required for correct anaphase and full APC/C activity in cells in culture

The above results indicate that maternally contributed CycB3 promotes mitotic anaphase in the early embryonic cell cycle. This is consistent with the observation that RNAi silencing of CycB3 delays mitotic anaphase in syncytial embryos [28]. Since *CycB3* mutants were found to be viable and develop normally until adulthood, any potential role of CycB3 during mitosis in proliferating cells may have been overlooked. By contrast, although *CycB* mutants are also viable, roles have been reported for CycB in *Drosophila* cell division [43,44]. Moreover, CycB3 is expressed specifically in proliferating cells, and *CycB3* is required for viability when *CycB* is mutated, with double mutants displaying strong mitotic defects [31]. To examine mechanistically how CycB3 contributes to mitotic regulation during divisions of proliferating cells, we

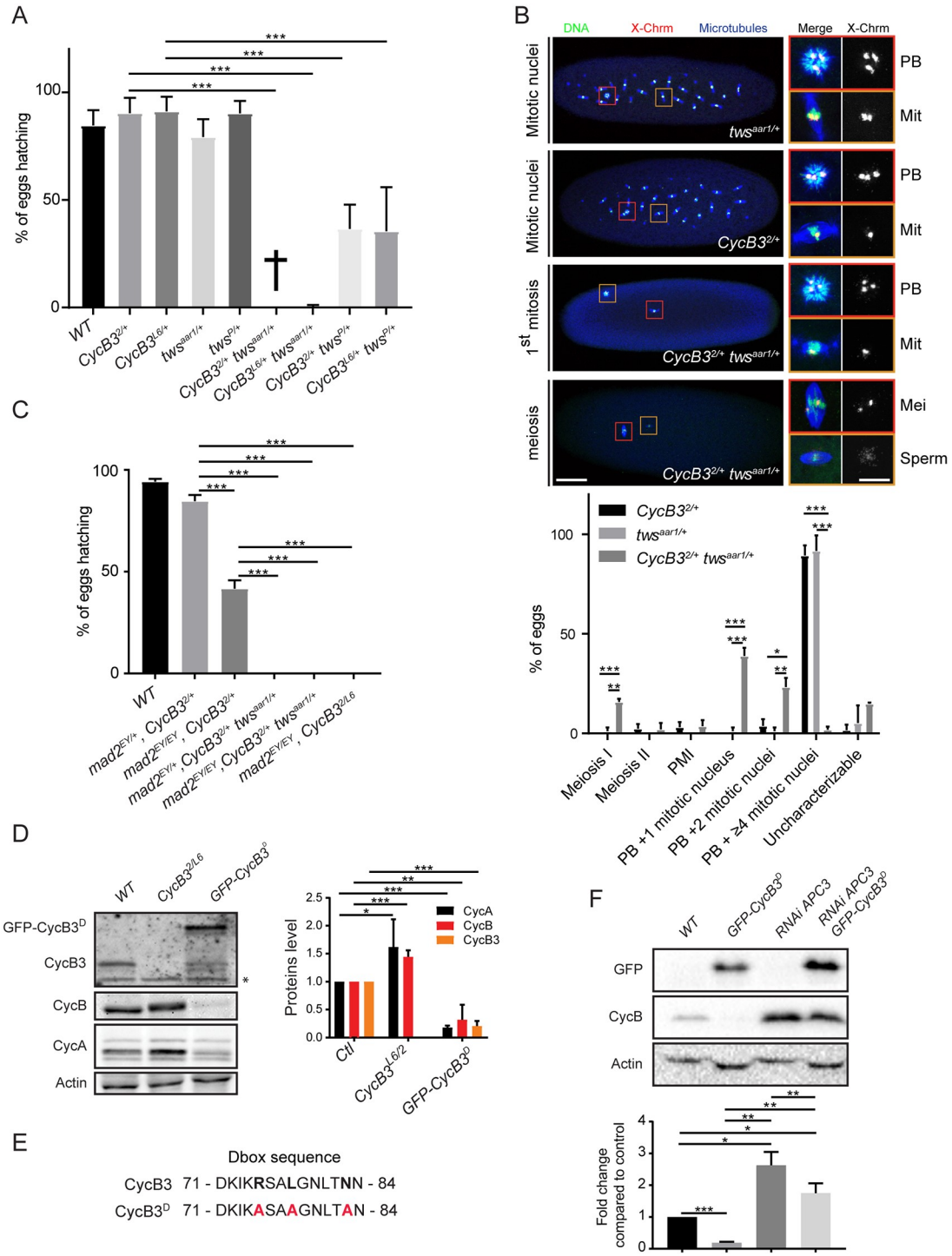

Fig 1. CycB3 collaborates with PP2A-Tws and functions upstream of the APC/C to promote the metaphase-anaphase transition in meiosis and mitosis. A. Mutations in *CycB3* and *tws* enhance each other in a maternal effect. Eggs from mothers of the indicated genotypes were scored for their hatching rate. B. Eggs from $CycB3^{2/+}$ $tws^{aar1/+}$ mothers arrest in metaphase of meiosis or mitosis. Green: DNA, Blue: α-Tubulin, Red: FISH for pericentric DNA of the X chromosome. Mitotic spindles (Mit) are recognized by the presence of astral microtubules, co-occurrence with a polar body (PB), and 1 or 2 foci of pericentromeric X-chromosome DNA. Meiotic I metaphase spindles (Mei) are recognized by the absence of astral microtubules, the absence of a polar body in the egg, and at least 2 foci of pericentromeric X-chromosome DNA. In a meiotic arrest, the sperm nucleus can break and nucleate a spindle (bottom images). Insets from the left are enlarged on the right with corresponding color frames. Scale bars: left panel 50 μm, right panel 10 μm. PMI: post-meiotic interphase. C. Inactivation of the SAC by mutation of *mad2*

does not rescue the development of embryos from *CycB3*$^{2/L6}$ or *CycB3*$^{2/+}$ *tws*$^{aar1/+}$ mothers. Eggs from mothers of the indicated genotypes were scored for their hatching rate. D. Mutation of *CycB3* results in higher CycA and CycB levels, while maternal expression of GFP-CycB3^{D} results in lower CycA, CycB and endogenous CycB3 levels in eggs. WT (Wild type): non-fertilized eggs. *Non-specific band. E. Mutation of the destruction box motif in CycB3^{D}. F. CycB3 negatively regulates CycB levels in an APC-dependent manner. Eggs were collected for 2 hrs from the indicated conditions and analyzed by Western blot. Expression of *UASp-GFP-CycB3*^{D} and of *UASp-APC3 RNAi* was driven maternally by *Mat α-Tubulin Gal4-VP16*. The *UASp-GFP-CycB3*^{D} and *UASp-APC3 RNAi* alone genotypes also contained a *UASp-WHITE* construct, to control for potential dilution of Gal4. Eggs from all conditions failed to develop (WT: unfertilized eggs). Error bars: SD. $^{***}p < 0.001$; $^{**}p < 0.01$; $^{*}p < 0.05$ from ANOVA for panels A and C and from paired *t*-tests for panels B, D and F. Numbers underlying graphs are available in supplemental file S1 Fig Numerical Data. See also S1 Fig.

https://doi.org/10.1371/journal.pgen.1009184.g001

used cells in culture. We generated D-Mel (d.mel-2) cells expressing H2A-RFP and Lamin-GFP, allowing us to measure the time between Nuclear Envelope Breakdown (NEB, T_0) and anaphase onset. To silence CycB3, we tested 4 different dsRNAs, and chose dsRNA no 1 and 2 because they resulted in the most efficient depletion of CycB3 (S2A Fig). We found that silencing CycB3 delays anaphase entry (Fig 2A, S1 and S2 Movies). This is observed by a delay in the cumulative percentage of cells entering anaphase after NEB, with both CycB3 dsRNA 1 or 2 (Fig 2B and S2B Fig). In addition, while control RNAi cells all enter anaphase within 3 hrs after NEB, 20% (dsRNA 1) and 13% (dsRNA 2) of the CycB3-depleted cells were still arrested in metaphase after 3 hrs.

Of the CycB3-depleted cells that do enter anaphase, a large proportion develop defects (Fig 2C and S2C Fig). The frequencies of lagging chromosomes and post-mitotic multinucleation/micronucleation approximately double relative to control cells. Interestingly, CycB3-depleted cells that do not enter anaphase sometimes undergo cytokinesis through a mass of unsegregated chromosomes (Fig 2A, arrow, S2 Movie). This is consistent with the previously observed role of CycB3 in negatively regulating cytokinetic furrowing [45].

To determine if the anaphase delay and defects resulting from CycB3 silencing correlate with reduced APC/C activity, we monitored the levels of CycB, an essential target of the APC/C during mitotic exit. Our previous results showed that CycB levels are regulated by CycB3 in eggs (Fig 1D and 1F, S1A and S1B Fig). We generated cells expressing CycB-GFP and Lamin-RFP, and measured CycB-GFP levels during mitosis. CycB-GFP is nuclear in prophase and becomes enriched on centrosomes and kinetochores until metaphase. We found that when CycB3 is depleted, CycB-GFP is degraded more slowly during the metaphase-anaphase transition, compared to control cells (Fig 2D and 2E, S3 and S4 Movies). In both conditions, anaphase onset occurs in the presence of similar CycB-GFP levels, suggesting that APC/C activity is rate-limiting for anaphase onset when CycB3 is depleted. Very similar results are obtained with a second dsRNA against CycB3 (S2D Fig). Interestingly, while CycB-GFP is not detected on particular structures in cells undergoing cytokinesis after anaphase, it persists on centrosomes and chromosomes in CycB3-depleted cells that undergo cytokinesis without anaphase (Fig 2D and S5 Movie).

We conclude that CycB3-dependent activation of the APC/C at the metaphase-anaphase transition is not restricted to female meiosis and the following syncytial embryonic mitotic cell cycles, but that it can also promote correct chromosome segregation during cell proliferation.

CycB3 associates with the APC/C and is spatially regulated during the cell cycle

The above results demonstrate that CycB3 promotes APC/C activation. To begin exploring if this regulation is direct, we tested if CycB3 associates with the APC/C. We used D-Mel cells expressing tagged proteins to perform co-purifications experiments. We found that CycB3-PrA specifically co-purifies Myc-APC3 (Fig 3A). Very similar results are obtained with

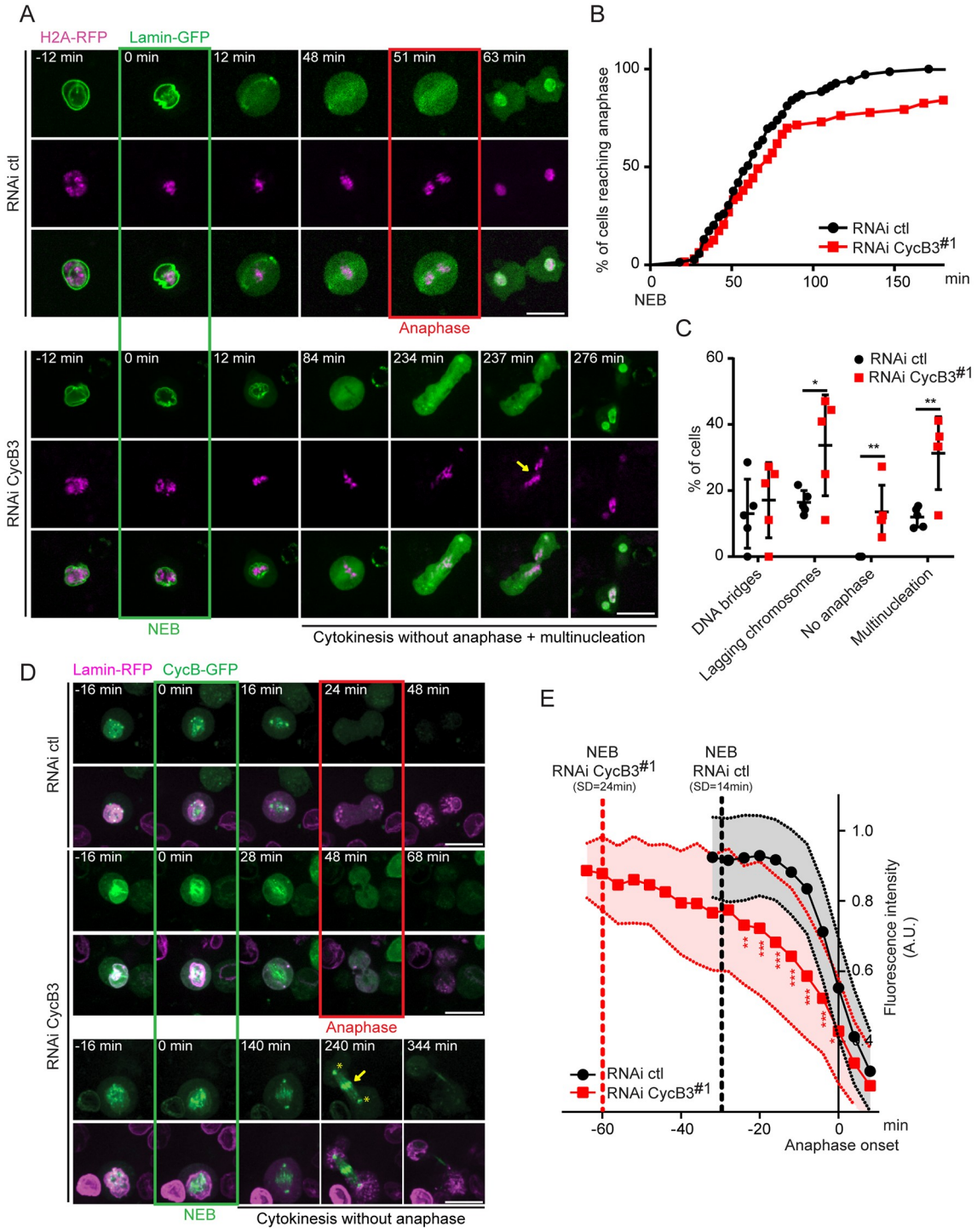

Fig 2. CycB3 is required for normal metaphase-anaphase transition and for CycB degradation in cells in culture. A. RNAi depletion of CycB3 delays anaphase entry and results in chromosome segregation defects in D-Mel cells. Note the cut through unsegregated chromosomes in this no-anaphase phenotype (arrow). RNAi ctl = transfection of dsRNA made from the bacterial KAN gene. B. Cumulative proportion of mitotic cells entering anaphase as a function of time after NEB. C. Frequency of cell division defects observed. Error bars: SD. For B-C, 63 and 69 cells were analyzed for RNAi CycB3 and ctl, respectively. D. RNAi depletion of CycB3 delays CycB degradation at the metaphase-anaphase transition. Examples of cell divisions are shown (Z-projection of 3 planes in focus through the nucleus). Note the abnormal persistence of CycB-GFP on the chromosomes (arrow) and centrosomes (asterisks) during cytokinesis in a cell that does not enter anaphase (bottom). E. Levels of CycB-GFP were quantified through time, relative to anaphase onset. 29 and 30 cells were analyzed for RNAi CycB3 and ctl, respectively. Error areas: SD. $^{***}p < 0.001$; $^{**}p < 0.01$; $^{*}p < 0.05$ from paired *t*-tests. Scale bars: 10 μm. Numbers underlying graphs are available in supplemental file S2 Fig Numerical Data. See also S2 Fig.

https://doi.org/10.1371/journal.pgen.1009184.g002

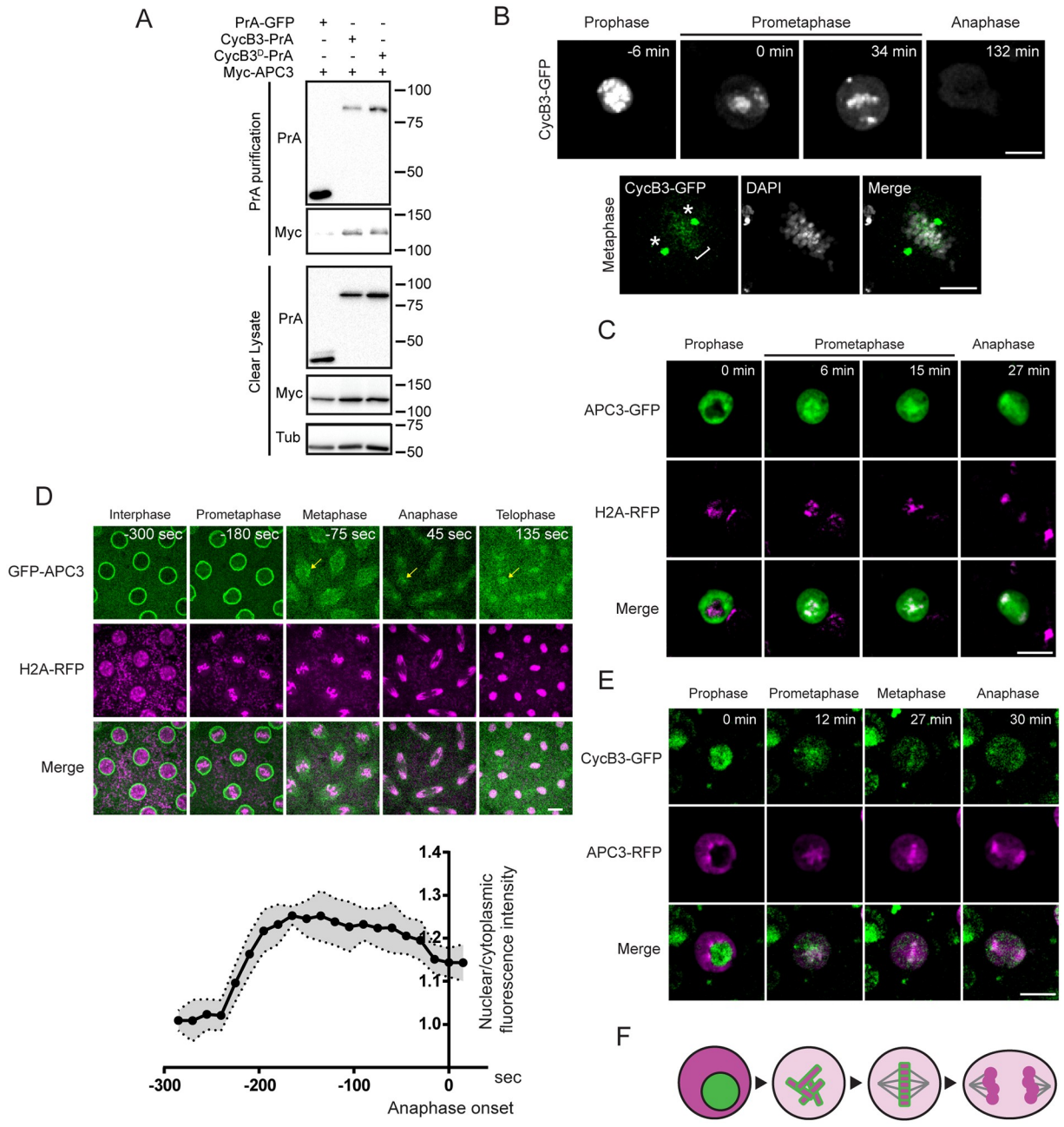

Fig 3. CycB3 associates with the APC/C and shows a dynamic localization relative to the APC/C in the cell cycle. A. Myc-APC3 associates with CycB3-PrA independently from its destruction box. Cells expressing the indicated proteins were submitted to Protein A affinity purification and products were analyzed by Western blot. B. CycB3-GFP localizes to chromosomes (bracket) and spindle poles (asterisks) in early mitosis. Top: Live imaging; Bottom: a fixed cell in metaphase. C. APC3-GFP is predominantly cytoplasmic in interphase and becomes enriched on chromosomes during mitosis in D-Mel cells. D. In syncytial embryos, GFP-APC3 becomes enriched in nuclei during mitotic entry and concentrates around the metaphase plate during mitosis (arrows). Scale bar: 10 μm. Bottom: quantification of the nuclear/cytoplasmic ratio of GFP-APC3 fluorescence intensity as nuclei enter mitosis. Averages between 10 nuclei of the same embryo are shown. Error area: SD. E. CycB3-GFP and APC3-RFP are sequestered from each other in interphase and come together on chromosomes in mitosis in D-Mel cells. Scale bars: 10 μm except for the fixed cell: 5 μm. F. Schematic model of the dynamic localization of CycB3 (green) and the APC/C (magenta) from interphase to anaphase. Numbers underlying graph are available in supplemental file S3 Fig Numerical Data. See also S3 Fig.

https://doi.org/10.1371/journal.pgen.1009184.g003

Myc-APC2 (S3A Fig). An interaction between CycB3 and the APC/C could occur as CycB3-Cdk1 binds the APC/C to phosphorylate it, or as CycB3 is recognized through its destruction box for ubiquitination by the APC/C. To discriminate between these modes of interaction, we used the destruction box mutation in CycB3. CycB3^{D}-PrA is still able to co-purify Myc-APC3 or Myc-APC2 (Fig 3A and S3A Fig), suggesting that the association observed does not reflect CycB3 binding as a substrate by the APC/C. We also found that CycB3-Myc can co-purify GFP-APC3 and GFP-APC6 in syncytial embryos (S3B and S3C Fig). Thus, CycB3 physically associates with the APC/C in D-Mel cells and in syncytial embryos, possibly to directly regulate the APC/C.

If CycB3 binds and directly activates the APC/C for the metaphase-anaphase transition, CycB3 and the APC/C should overlap in localization before anaphase. We investigated the spatio-temporal regulation of CycB3 relative to the APC/C using D-Mel cells. CycB3 overexpression appears to be toxic as it was difficult to obtain stable cell lines expressing CycB3 fused to any tag. Cells expressing the highest levels of CycB3-GFP tended not to divide. Nevertheless, we managed to film divisions of cells expressing enough CycB3-GFP to reveal its dynamic localization. CycB3-GFP is strongly nuclear in interphase until prophase and becomes enriched on condensed chromosomes and on centrosomes as cells enter mitosis and until metaphase (Fig 3B and S6 Movie). Starting in anaphase, CycB3-GFP levels are rapidly reduced, consistent with its degradation by the APC/C. Contrary to CycB3-GFP which is nuclear, APC3-GFP is strongly cytoplasmic in interphase until prophase. After NEB, APC3-GFP quickly becomes enriched on condensed chromosomes (marked by H2A-RFP) until telophase (Fig 3C). In syncytial embryos, GFP-APC3 shows similar spatial dynamics, becoming enriched in the nuclei during mitotic entry and concentrated around the metaphase plate (marked by H2A-RFP) during mitosis, with an additional strong localization to nuclear envelopes (Fig 3D and S7 Movie). This pattern is consistent with previous observations with GFP-APC3 alone [46]. We were able to generate a stable cell line where a fraction of the cells co-express detectable levels of CycB3-GFP and APC3-RFP. Examination of these cells confirms that nuclear CycB3-GFP and cytoplasmic APC3-RFP are mutually sequestered in interphase until NEB, and subsequently become co-enriched on or around chromosomes (Fig 3E and 3F, S8 Movie).

Altogether, these results suggest that CycB3 interacts with the APC/C on chromosomes, to promote APC/C activation before anaphase. The physical separation between CycB3 and the APC/C in interphase may safeguard against premature APC/C activation.

CycB3 promotes APC/C phosphorylation at CDK motifs and interaction with Cdc20 co-activators

The only known molecular function of *Drosophila* CycB3 is to bind and activate Cdk1. Thus, we next sought to determine if CycB3, in complex with Cdk1, promotes the activation of the APC/C by direct phosphorylation. To this end, we used syncytial embryos, where mitoses occur approximately every 10 min, thereby facilitating the detection of mitotic complexes and mitotic phosphorylation. We used fly lines expressing APC3/Cdc27 and APC6/Cdc16 N-terminally fused with GFP and expressed under the polyubiquitin promoter [46]. We collected early embryos from these flies and purified the APC/C using a GFP-affinity resin. The band patterns we obtained after purification of GFP-APC3 or GFP-APC6 are similar on a silver-stained gel, and different from those obtained after purification of GFP-tagged Nup107, a component of the nuclear pore complex (Fig 4A). Mass spectrometry analysis revealed the presence of most APC/C subunits in the GFP-APC/C purification products (S1 Table). Western blots detected endogenous CycB3 that co-purified specifically with GFP-tagged APC/C, compared with GFP-Nup107 used as a negative control (Fig 4B). Cdk1 was also enriched in the

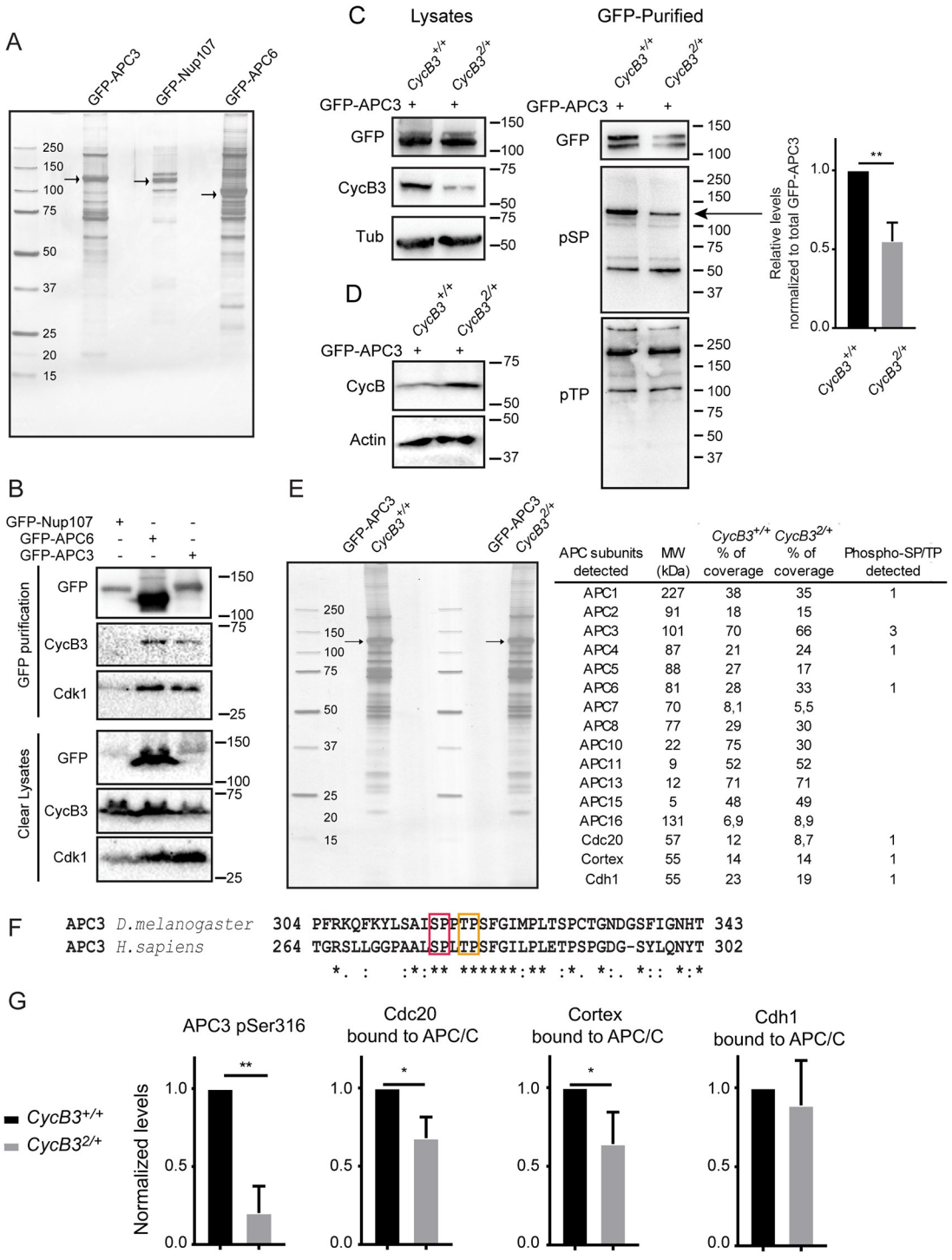

APC subunits detected	MW (kDa)	CycB3+/+ % of coverage	CycB3Δ2/+ % of coverage	Phospho-SP/TP detected
APC1	227	38	35	1
APC2	91	18	15	
APC3	101	70	66	3
APC4	87	21	24	1
APC5	88	27	17	
APC6	81	28	33	1
APC7	70	8,1	5,5	
APC8	77	29	30	
APC10	22	75	30	
APC11	9	52	52	
APC13	12	71	71	
APC15	5	48	49	
APC16	131	6,9	8,9	
Cdc20	57	12	8,7	1
Cortex	55	14	14	1
Cdh1	55	23	19	1

Fig 4. CycB3-Cdk1 physically associates with the APC/C and promotes its phosphorylation and interaction with Cdc20 co-activators. A. Embryos expressing GFP-APC3, GFP-APC6 and GFP-Nup107 were submitted to GFP-affinity purification and purified complexes were visualized on a silver-stained gel. Arrows: GFP-tagged proteins. B. CycB3 physically associates with the APC/C in embryos. Embryos expressing the indicated proteins were submitted to GFP-affinity purification and products were analyzed by Western blots. C. APC/C phosphorylation at SP site(s) is CycB3-dependent. GFP-affinity purifications were conducted from 0–2 hrs-old GFP-APC3 expressing embryos from *CycB3*$^{+/+}$ and *CycB3*$^{2/+}$ mothers and products were analyzed by Western blots. Left: Western blots on lysates used in the purifications. Note that CycB3 levels are lower in *CycB3*$^{2/+}$ embryos; Center: GFP-APC3 purified products were analyzed by Western blot with antibodies against pSP or pTP sites (minimal CDK phosphorylation motifs). Arrow: presumed GFP-APC3 pSP band, less intense in *CycB3*$^{2/+}$ embryos. Right: relative intensities of

the band indicated by the arrow, after normalization to the amounts of total GFP-APC3 purified. Error bar: SD for 3 experiments. $^{**}p = 0.0082$ from paired *t*-test. D. Western blot showing that CycB levels are higher in $CycB3^{2/+}$ embryos (aged 0–2 hrs). E. Purification of the APC/C complex using GFP-APC3 from $CycB3^{+/+}$ and $CycB3^{2/+}$ embryos, for mass spectrometry analysis. Table: APC/C subunits detected by mass spectrometry. Their predicted molecular weight (MW), percentage of sequence detected and number of phospho SP/TP sites detected are indicated. F. Phosphorylation sites at minimal CDK motifs identified in *Drosophila* APC3 are conserved in the activation loop of human APC3. Red box: Ser316; Orange box: Thr319. G. Phosphorylation at Ser316 in APC3 is reduced in $CycB3^{2/+}$ embryos. In addition, the amounts of Cdc20/Fizzy and Cortex co-purified with the APC/C are reduced in $CycB3^{2/+}$ embryos. The amount of Cdh1/Fzr co-purified is not significantly affected. Proteins and phosphopeptides abundances relative to APC3 levels were normalized to 1 in the $CycB3^{+/+}$ condition (see Methods). Error bars: SD for 3 experiments. Numbers underlying graphs are available in supplemental file S4 Fig Numerical Data.

https://doi.org/10.1371/journal.pgen.1009184.g004

GFP-APC/C purification products. Therefore, endogenous CycB3 and Cdk1 associate with the APC/C in early embryos.

We then used phosphospecific Western blotting to explore whether the phosphorylation state of the APC/C depends on CycB3. For these experiments, we sought to compare the phosphorylation levels of purified APC/C from embryos laid by females wild-type for *CycB3* or heterozygous for the $CycB3^{2}$ null allele. In embryos from $CycB3^{2/+}$ mothers, the level of CycB3 is approximately halved, as expected (Fig 4C). Our genetic results indicate that this reduction in CycB3 levels causes metaphase arrests in the context of heterozygosity for *tws* (Fig 1A and 1B), suggesting that APC/C activation may be substantially weakened. Consistent with this idea, CycB levels are higher in embryos from $CycB3^{2/+}$ mothers (Fig 4D). We then purified the APC/C via GFP-APC3 and submitted the products to Western blots using phosphospecific antibodies against pSP or pTP sites, which are the minimal motifs for CDK phosphorylation. The anti-pSP blot reveals several bands (Fig 4C, center). After quantifications that included a correction to take into account slight variations in amounts of GFP-APC3 purified, we found only one pSP band that is significantly less intense in purified products from $CycB3^{2/+}$ embryos (Fig 4C, arrow, quantified on right). This pSP band is the most intense in purification products from $CycB3^{+/+}$ embryos, and its molecular mass of 125 kDa matches that observed for GFP-APC3. This result suggests that CycB3 is required for APC3 phosphorylation at CDK sites.

We set out to test this hypothesis directly using quantitative mass spectrometry. We repeated the purification of GFP-APC3 in both genotypes on a larger scale. Very similar amounts of APC/C were purified from $CycB3^{2/+}$ or $CycB3^{+/+}$ embryos, with similar band profiles detected on a gel (Fig 4E). We detected 3 phosphorylated sites at minimal CDK motifs in APC3, including S316 and T319. Both sites are conserved in human APC3, and map within the loop whose phosphorylation promotes APC/C activation. Moreover, both sites in human APC3 (S276 and T279) were shown to be phosphorylated *in vivo*, and by Cyclin A3-Cdk2 *in vitro* (Fig 4F) [19,47]. From the mass spectrometry data, we measured the relative abundances of APC3 phosphopeptides compared to unphosphorylated APC3 peptides in the same purification products. We found that phosphorylation at S316 is strongly reduced in $CycB3^{2/+}$ embryos vs $CycB3^{+/+}$ embryos, suggesting that it is regulated by CycB3-Cdk1 (Fig 4G). Phosphorylation at T319 was too weak to be quantified by the same method. In addition, the Western blot with the anti-pTP reveals no obvious difference between $CycB3^{2/+}$ and $CycB3^{+/+}$ embryos (Fig 4C), suggesting that pTP sites on the APC/C are not major points of regulation by CycB3. The third site we identified, S455, does not change in intensity of phosphorylation between genotypes (S4 Fig Numerical Data).

CDK phosphorylation of APC3 is an essential part of a mechanism for APC/C activation demonstrated *in vitro* [19,20]. This event primes the APC/C for its CDK phosphorylation of APC1, which results in the displacement of a switch loop within APC1, opening the binding site for Cdc20. There are three Cdc20 paralogs in *Drosophila*: Fizzy/Cdc20 that activates the

APC/C in mitosis and meiosis [40–42,48], Cortex that activates the APC/C in female meiosis and possible syncytial mitoses [40,42], and Cdh1 which is not detected in syncytial embryos and keeps the APC/C active in G1 in later developmental stages [49]. To test the idea that CycB3 promotes APC binding to its co-activators, we determined the relative amounts of Cdc20, Cortex and Cdh1 in GFP-APC3 purification products from *CycB3*$^{2/+}$ and *CycB3*$^{+/+}$ embryos. Cdc20, Cortex and Cdh1 are all detected in association with the APC/C purified from embryos aged from 0–2 hrs (Fig 4E). The presence of Cdh1 may be surprising but it could come from the oldest embryos collected that may have initiated the maternal-zygotic transition. Strikingly, the relative levels of both Cdc20 and Cortex are lower in the GFP-APC3 purification products from *CycB3*$^{2/+}$ embryos compared with *CycB3*$^{+/+}$ embryos (Fig 4G). However, Cdh1 levels are unchanged. These results suggest that CycB3 specifically promotes APC/C recruitment of its mitotic and meiotic co-activators Cdc20 and Cortex.

Mechanism and conservation of the role of Cyclin B3 in the activation of the APC/C

Altogether, our results strongly suggest that CycB3-Cdk1 directly activates the APC/C by phosphorylation, promoting its function at the metaphase-anaphase transition in meiosis and in both maternally driven early embryonic mitoses and somatic cell divisions. This regulation is likely mediated by the phosphorylation in the activation loop of APC3 by CycB3-Cdk1 that ultimately promotes the recruitment of the Cdc20-type co-activators Fizzy and Cortex (Fig 5). Previous work has shown that APC3 phosphorylation and APC/C activation by cyclin-CDK complexes require their CKS subunit [19,50,51]. CKS subunits can act as processivity factors that bind phosphorylated sites to promote additional phosphorylation by the CDK [52,53]. Thus, phosphorylation of APC3 would prime the binding of a cyclin-CDK-CKS complex to promote the additional phosphorylation of APC1, allowing for Cdc20 binding [19]. It has been shown that mutation of phosphorylation sites into Asp or Glu residues cannot substitute for the presence of phosphate in the CKS binding site [54]. Therefore, it was not possible to

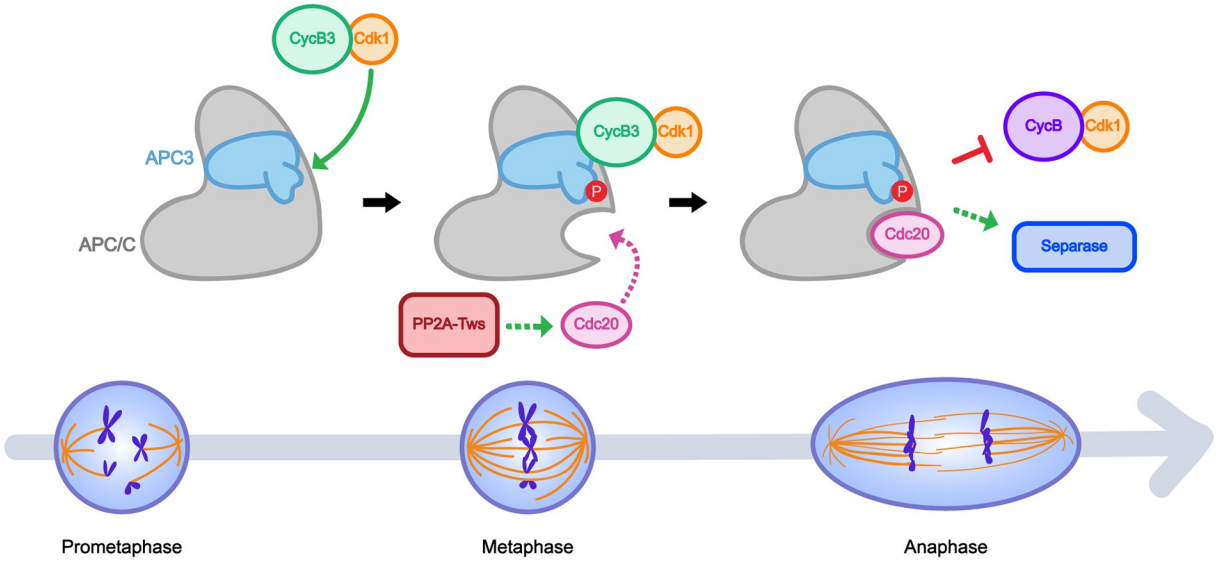

Fig 5. Model for APC/C activation by CycB3-Cdk1 in meiosis and mitosis. CycB3-Cdk1 binds the APC/C and phosphorylates its APC3 subunit. This event promotes the binding of Cdc20 co-activators, likely through known mechanisms [19,20]. In addition, PP2A-Tws may help Cdc20 recruitment to the APC/C [15,17]. Activated APC/C triggers CycB degradation, separase activation and anaphase.

https://doi.org/10.1371/journal.pgen.1009184.g005

generate a mutation in APC3 that would have mimicked phosphorylation at S316 to enhance cyclin-CDK-CKS binding. Such a mutation in APC3, if it were possible, would have potentially rescued APC/C activity in the absence of CycB3 according to our model. However, it is likely that our analysis did not detect all phosphorylation sites in the APC/C. Thus, we cannot exclude the possibility that other phosphorylation events, mediated by CycB3-Cdk1 or another kinase, may be required for complete APC/C activation. For example, other phosphorylation events have been proposed to regulate APC/C localization [55]. It is even formally possible that CycB3-Cdk1 is required to activate another proline-directed kinase that phosphorylates APC3 at S316. The interdependence between CycB3 and Tws that we uncovered may reflect a role of PP2A-Tws in the recruitment of Cdc20 co-activators to the APC/C. Cdc20 must be dephosphorylated at CDK sites before binding the APC/C, and in human cells both PP2A-B55 and PP2A-B56 promote this event [15–17].

CycB3 is strongly required for APC/C activation in meiosis and in the early syncytial mitoses, and to a lesser extent in other mitotic divisions, despite the presence of two additional mitotic cyclins, CycA and CycB, capable of activating Cdk1. There are many possible reasons for this requirement. Overexpression of stabilized forms of CycA or CycB can block or slow down anaphase, suggesting that they may interfere with APC/C function in this transition [56]. However, under normal expression levels, CycA or CycB or both may contribute to activate the APC/C like CycB3. *CycB3* mutant flies develop until adulthood [31], which implies that the APC/C can be activated to induce anaphase in at least a vast proportion of mitotic cells, and this activation could be mediated by CycA and/or CycB. *CycA* is essential for viability and *CycB* mutants show strong female germline development defects, complicating the examination of potential roles for these cyclins at the metaphase-anaphase transition [29,31,32,44]. Thus, in principle, the requirements for CycB3 in female meiosis, in embryos and in mitotic cells in culture could merely reflect the need for a minimal threshold of total mitotic cyclins. We consider this possibility unlikely because CycB3 is expressed at much lower levels than CycB in early embryos [57]. Moreover, while maternal heterozygosity for mutations in *CycB3* and *tws* causes a metaphase arrest in embryos (Fig 1), heterozygosity for mutations in *CycB* and *tws* does not cause embryonic defects [37]. In fact, genetic results suggest that the function of CycB is antagonized by PP2A-Tws in embryos, while CycB3 and PP2A-Tws collaborate for APC/C activation in embryos [37]. Thus, although it is possible that CycA and CycB can participate in APC/C activation, CycB3 probably has some unique feature that makes it particularly capable of promoting APC/C activation.

By what mechanism could CycB3 be particularly suited for APC/C activation? Cyclins can play specific roles by contributing to CDK substrate recognition or by directing CDK activity in space and time [58]. We did not investigate the precise nature of the molecular recognition of the APC/C by CycB3. It may be that CycB3 possesses a specific binding site for the APC/C that is lacking in CycA and CycB. Another possibility is that differences in localization between cyclins dictate their requirements. In particular, while CycA and CycB are cytoplasmic in interphase, CycB3 is nuclear [31]. We surmise that the nuclear localization of CycB3 may help concentrate CycB3 in the spindle area upon germinal vesicle breakdown, when the very large oocyte enters meiosis. In future studies, it will be interesting to compare the ability of different mitotic cyclins to activate the APC/C and to determine the molecular basis of potential differences.

In any case, our results show that CycB3 activates the APC/C and that this regulation is essential in *Drosophila*. Cyclin B3 has been shown to be required for anaphase in female meiosis of insects (*Drosophila*), worms (*C. elegans*) and vertebrates (mice). It is tempting to conclude that the activation of the APC/C is a function of Cyclin B3 conserved in all these species. However, in *C. elegans* embryos, the metaphase arrest upon CYB-3 (Cyclin B3) inactivation requires SAC activity [36]. The underlying mechanism and whether it also occurs in other

systems remain to be determined. However, CYB-3 plays roles in *C. elegans* that have not been detected for Cyclin B3 in flies or vertebrates, including a major role in mitotic entry, where CYB-3 mediates the inhibitory phosphorylation of Cdc20 [59]. In this regard, *C. elegans* CYB-3 may be more orthologous to Cyclin A. Yet, given that Cyclin B3 is required for anaphase in a SAC-independent manner in flies and mice, it seems reasonable to suggest that the direct activation of the APC/C by Cyclin B3 is conserved in vertebrates.

Materials and methods

All numerical data underlying the figures are available as supplementary files.

Plasmids and mutagenesis

Plasmids were generated using the Gateway recombination system (Invitrogen). Coding sequences were first cloned into a pDONOR221 entry vector. Then, they were recombined into the relevant destination vectors for expression under either the copper-inducible (pMT) or constitutive (pAC5) promoters. The following expression vectors were generated: pAC5-CycB-GFP, pAC5-CycB3-GFP, pMT-CycB3-GFP, pAC5-PrA-GFP, pAC5-CycB3-PrA, pAC5-CycB3^{D}-PrA, pAC5-Myc-APC3, pAC5-Myc-APC2, pMT-APC3-GFP, pMT-APC3-RFP, pMT-H2A-RFP, pMT-Lamin-RFP and pAC5-Lamin-GFP. For CycB3^{D}, the mutagenesis was performed using *PFU* DNA Polymerase (Biobasic) according to the manufacturer's instructions.

Fly genetics

Fly culture was done according to standard procedures. All crosses were performed at 25˚C. The WT strains used were W^{1118} and *Oregon R*. Transgenic flies for the expression of pUASp-CycB3-Myc and pUASp-GFP-CycB3^{D} were generated by random insertion.

The Bloomington *Drosophila* Stock Center (BDSC) provided the following fly lines for RNAi: White^{GL00094} (35573), APC1^{HMS01744} (38531), APC3^{HMC03814} (55155); for mutant alleles: $CycB3^{2}$ (6635), $CycB3^{L6}$ ($CycB3^{L6540}$; 10337), $mad2^{EY21687}$ (22495), $cort^{QW55}$(4974), $cort^{RH65}$(77860) and *C(1)M3*, y^{2}/*C(1;Y)1*, y^{1}/*0* (38416); for transgenic insertions: *GFP-Nup107* (35514), and for drivers: *matα4-GAL-VP16* (7062) and *otu-Gal4-VP16* (58424). Fly strains harboring the $CycB3^{2}$ and $CycB3^{L6}$ alleles and the GFP-Nup107 insertion were from the BDSC. The tws^{P} and tws^{aar1} alleles were obtained from David Glover. The fzy^{6} and fzy^{7} alleles were obtained from Ian Dawson. pUb-GFP-APC3 and pUb-GFP-APC6 lines were provided by Yuu Kimata and were previously described [46].

To generate $cort^{QW55/RH6}$, $fzy^{6/7}$ double mutant females, $cort^{QW55}$ was recombined with fzy^{6} and $cort^{RH65}$ was recombined with fzy^{7}. Crosses to generate $cort^{QW55/RH65}$, $fzy^{6/7}$ double mutants were reared at 18˚C until pupation and then moved to 29˚C. Wild type unfertilized eggs were generated by crossing wild type females to X/O males. X/O males were generated by crossing *X^Y (C(1)M3*, y^{2}/*C(1;Y)1*, y^{1}/*0*) males to wild type females.

Expression of *UASp* transgenes in the female germline and early embryo were done with *matα4-GAL-VP16* in Fig 1A and 1C and S1A Fig, and with *otu-Gal4-VP16* in S1B Fig.

For fertility tests, between 5 and 10 individual females were crossed with 3 males and allowed to lay eggs for 1 day on grape juice agar tubes with yeast paste before being removed. The percentage of hatched eggs was counted 24 h later.

Drosophila cell culture and transfections

All cells were in the D-Mel (d.mel-2) background and were cultured in Express Five medium supplemented with glutamine, penicillin, and streptomycin. All stable cell lines were selected

in medium containing 20 μg/ml blasticidin. Expression of the pMT constructs was induced with 300 μM $CuS0_4$ overnight.

Plasmid transfections were performed using X-tremeGENE HP DNA Transfection Reagent (Roche). For RNA interference, cells were transfected using Transfast reagent in six-well plates with 30 μg of dsRNA against CycB3 or control. The control dsRNA was generated against the sequence of the bacterial kanamycin resistance gene (*KAN*). Cells were analyzed 48 h later by immunoblotting or live-cell imaging.

Protein purifications

Protein A affinity purifications from D-Mel cells were done largely as described [60]. Briefly, cells were co-transfectd with pAC5-CycB3-Pra and pAC5-Myc-APC2 or pAC5-Myc-APC3, harvested from confluent 75 cm^2 flasks and resuspended in 1.6 ml of lysis buffer (50 mM Tris-CL pH 7.5, 150 mM NaCl, 0.1 mM EGTA, 2 mM $MgCl_2$, 1 mM DTT, 1.5 μM aprotinin, 23 μM leupeptin, 1 mM PMSF, 10% glycerol, 0.5% triton X-100) supplemented with protease inhibitors. Lysates were clarified by centrifugation at 10 000 g for 15 min in a tabletop centrifuge at 4˚C. Supernatants were incubated for 1 h at 4˚C with 25 μl of DynaBeads previously conjugated to rabbit IgG. Beads were washed five times with 1 ml of lysis buffer for 5 min at 4˚C. Purification products were eluted by heating at 95˚C for 5 min in Laemmli buffer and analyzed by Western blotting.

For protein immunopurifications from egg/embryos, 0–2 h collections were performed at 25˚C. Eggs were dechorionated in 50% bleach, then washed in PBS and frozen in liquid nitrogen. 100 mg of embryos were crushed in lysis buffer as above. Lysates were incubated for 30 min at 4˚C on a rotating wheel, and centrifugated at 10 000 g for 15 min. Lysates were then incubated with antibody (anti-Myc antibody 9E10 or anti-CycB3, from rabbit, custom-made by Genscript) for 1 hour. Then the lysate was incubated for 2 hours with PrG-coupled (for anti-Myc) or PrA-coupled magnetic beads (anti-CycB3). Beads were washed 5 times in lysis buffer followed by elution in Laemmli buffer at 95˚C for 5 min.

For GFP affinity purifications, embryos were crushed in the same lysis buffer as above but supplemented with 1% phosphatase inhibitor (Cocktail 2 (P5726) and 3 (P0044), Sigma). Lysates were incubated for 30 min at 4˚C on a wheel, and centrifugated at 10 000 g for 15 min. Lysates were then incubated with GFP-trap nanobeads (Chromotek) for 2 h. Beads were washed 5 times with lysis buffer. For mass spectrometry, 5 additional washes in PBS + protease inhibitors were performed. 90% of the sample was sent for mass spectrometry. The remaining 10% was eluted in Laemmli buffer and used for SDS-PAGE analysis by silver nitrate staining and Western blots.

Mass spectrometry

Protein purification products were analyzed by Liquid Chromatography—Mass Spectrometry (LC-MS). Samples were reconstituted in 50 mM ammonium bicarbonate with 10 mM TCEP [Tris (2-carboxyethyl) phosphine hydrochloride; Thermo Fisher Scientific], and vortexed for 1 h at 37˚C. Chloroacetamide (Sigma-Aldrich) was added for alkylation to a final concentration of 55 mM. Samples were vortexed for another hour at 37˚C. One microgram of trypsin was added, and digestion was performed for 8 h at 37˚C. Supernatants were desalted on stage-tips (The Nest Group). Samples were dried down and solubilized in 5% acetonitrile (ACN)-0.2% formic acid (FA). The samples were loaded on a home-made reversed-phase column (150-μm i.d. by 150 mm) with a 220-min gradient from 10 to 30% ACN-0.2% FA and a 600-nl/min flow rate on a Easy nLC-1000 connected to an Orbitrap Fusion (Thermo Fisher Scientific, San Jose, CA). Each full MS spectrum acquired at a resolution of 240,000 was followed by tandem-MS

(MS-MS) spectra acquisition on the most abundant multiply charged precursor ions for a maximum of 3s. Tandem-MS experiments were performed using collision-induced dissociation (CID) at a collision energy of 30%. The data were processed using PEAKS X (Bioinformatics Solutions, Waterloo, ON) and a Uniprot *Drosophila* unreviewed database. Mass tolerances on precursor and fragment ions were 10 ppm and 0.3 Da, respectively. Fixed modification was carbamidomethyl (C). Variable selected posttranslational modifications were oxidation (M), deamidation (NQ), phosphorylation (STY), acetylation (N-ter). The data were visualized with Scaffold 4.3.0. For measurements of relative abundances, first, areas under precursor peptide peaks from LC-MS spectra were obtained through PEAKS X quantitation mode. Normalization of peptide peak areas was performed for all LC-MS acquisitions from total ion current as a reference, to give raw abundance values (arbitrary units) for peptides to be quantified. For assessment of phosphorylation levels, raw abundances of all tryptic peptides phosphorylated at the site of interest were summed. For Cdc20, Cortex and Cdh1 levels, raw abundances of all detected peptides from these proteins were summed. In all cases, the resulting values were divided by the total raw abundance of the 3 most intense unmodified peptides from APC3 in the same samples. The resulting relative abundances were then normalized to set values at 1 in the *CycB3*$^{+/+}$ control condition (Fig 4G).

Western blotting and immunofluorescence

Primary antibodies used in Western blotting and immunofluorescence were anti-GFP from rabbit (TP401, Torrey Pines, at 1:2000 dilution for WB), anti-GFP from rabbit (A6455, Invitrogen, at 1:200 for IF), anti-CycA from mouse (A12 purified, Developmental Studies Hybridoma Bank, 1/1000), anti-CycB from mouse (F2F4 purified, Developmental Studies Hybridoma Bank, 1/2000), anti-CycB3 from rabbit (Custom-made by Thermo Fisher Scientific, at 1:2000 dilution for WB; except for Fig 1D, where a rabbit antibody provided by Christian Lehner was used), anti-B55 (tws) from rabbit (2290S, Cell Signaling, at 1:2000 for WB) anti-α-tubulin DM1A from mouse (#T6199, Sigma, at 1:10,000 dilution for WB), anti-Myc 9E10 from mouse (#sc-40, Santa Cruz Biotechnology, Inc., at 1:2000 dilution for WB), mouse monoclonal anti-actin (#MAB1501, Millipore, at 1/5000), anti-P-SP from rabbit (#9477, Cell Signaling, at 1:2000 dilution for WB in 5%BSA), anti-P-TP from rabbit (#14371, Cell Signaling, at 1:2000 dilution for WB in 5% BSA), anti-Cdk1 PSTAIR from mouse (#10345, Abcam, at 1:2000 dilution for WB), anti-α-tubulin YL1/2 from rat (MCA77G, Bio-Rad AbD Serotec, at 1:2000 dilution for IF), anti-rabbit Alexa Fluor 488 (A11008, Invitrogen, at 1/200 for IF), anti-rat Alexa Fluor 647 from goat (A21247, Invitrogen, at 1:1000 for IF), peroxidase-conjugated anti-mouse from goat (115-035-003, Jackson ImmunoResearch, at 1:5000 for WB), peroxidase-conjugated anti-rabbit from goat (111-035-008, Jackson ImmunoResearch, at 1:5000 for WB), peroxidase-conjugated ChromPure from Rabbit (011-030-003, Jackson ImmunoResearch, at 1:5000 for WB).

For Western blots from stage 14 oocytes, ovaries were dissected in Isolation Buffer (55 mM NaOAc, 40 mM KOAc, 110 mM sucrose, 1.2 mM MgCl2, 1 mM CaCl2, and 100 mM HEPES, pH 7.4) with collagenase to dissociate individual oocytes. Late stage oocytes were selectively enriched by repeated rinses in Isolation Buffer and removing slowly settling smaller egg chambers.

Microscopy

For immunofluorescence, cells were fixed on coverslips with 4% formaldehyde during 20 min at room temperature (RT). Cells were permeabilized and blocked in PBS containing 0.1% Triton X-100 and 1% BSA. Cells were incubated with primary antibodies diluted in PBS

containing 0.1% Triton (PBT) for 1 h at RT, washed three times in PBS and incubated with secondary antibodies and DAPI diluted in PBT for 1 h at RT. Then, coverslips were washed 3 times in PBS before being mounted in Vectashield medium (Vector Laboratories). Imaging was performed using a confocal system Zeiss LSM880.

For Fluorescence *In Situ* Hybridization (FISH), 0–2 h eggs were dechorionated in bleach and then washed 3 times in 0.7% NaCl, 0.05% Triton X-100). Eggs were then fixed in methanol:heptane (1:1) while shaking vigorously. Eggs were then stored at -20˚C for later use, or immediately rehydrated successively in 9:1, 7:3 and 1:1 methanol:PBS solutions. FISH was performed on methanol-fixed eggs as described [61], using a probe against the 359-base pair pericentromeric repeat on the X chromosome. DNA was stained with QUANT-IT Oligreen (#O7582, Invitrogen, 1/5000). Eggs were mounted using tetrahydronaphthalene. Imaging was performed using a confocal system Leica SP8.

For live analysis of *Drosophila* syncytial embryos, 0–2 h embryos were first dechorionated in 50% bleach, aligned on a coverslip and covered with halocarbon oil. 25 confocal sections of 1 μm were collected per time point for each embryo. Live imaging was performed using a Spinning-Disk confocal system Yokogawa CSU-X1 5000 mounted on a fluorescence microscope (Zeiss Axio Observer.Z1). Images were treated using Zen software (Zeiss) and Fiji software (NIH) as described [62].

To film D-Mel cells, they were plated on a LabTek II chambered coverglass (#155409, Thermo Fisher Scientific) and imaging was performed using the same Spinning-Disk microscope as for embryos. To monitor CycB-GFP levels, GFP fluorescence signal in the whole cell was quantified directly with the Zen software. To measure the GFP fluorescence ratio, time-lapse images were collected at 3 min intervals for H2A-RFP Lamin-GFP cells or 4 min intervals for Lamin-RFP CyclinB-GFP cells. For each timepoint, a circle was drawn in a single in-focus plane at the level of chromosomes and the whole intensity was measured. A ratio was then calculated between each timepoint value and the first timepoint value.

Supporting information

S1 Table. APC subunits and co-activators detected by mass spectrometry in the purification products shown in Fig 4A.
(XLSX)

S1 Fig. CycB3 promotes APC/C activity in eggs (related to Fig 1). A-B. CycB3 negatively regulates CycB levels in an APC-dependent manner. Eggs were collected for 2 hrs from the indicated conditions and analyzed by Western blot. In A, expression of *UASp-GFP-CycB3^{D}* and of *UASp-APC1 RNAi* was driven maternally by *Mat α-Tubulin Gal4-VP16*. The *UASp-GFP-CycB3^{D}* and *UASp-APC1 RNAi* alone genotypes also contained a *UASp-WHITE* construction, to control for potential dilution of Gal4. Eggs from all conditions failed to develop (Ctl: unfertilized eggs). In B, expression of *UASp-GFP-CycB3^{D}* was driven maternally by *otu-Gal4-VP16*. Error bars: SD. $^{**}p < 0.01$; $^{*}p < 0.05$ from paired *t*-tests. Numbers underlying graphs are available in supplemental file S1 Fig Numerical Data.
(TIF)

S2 Fig. CycB3 promotes APC/C activity in mitosis in D-Mel cells (related to Fig 2). A. dsRNAs targeting different regions of the CycB3 transcript were tested. No 1 and 2 were more effective and selected for experiments. B-D. Similar results were obtained with dsRNA no 2 (here), compared with dsRNA no 1 (Fig 2). B-C. RNAi ctl: 106 cells; RNAi CycB3: 107 cells analyzed. D. RNAi ctl: 30 cells; RNAi CycB3: 40 cells analyzed. Error areas and error bars: SD. $^{***}p < 0.001$; $^{**}p < 0.01$; $^{*}p < 0.05$ from paired *t*-tests. Scale bars: 10 μm. Numbers underlying

graphs are available in supplemental file S1 Fig Numerical Data.
(TIF)

S3 Fig. CycB3 associates with the APC/C (related to Fig 3). A. Myc-APC2 associates with CycB3-PrA independently from its destruction box. Cells expressing the indicated proteins were submitted to Protein A affinity purification and products were analyzed by Western blot. B-C. CycB3-Myc co-purifies GFP-APC3 (B) or GFP-APC6 (C) in *Drosophila* syncytial embryos.
(TIF)

S1 Movie. Normal mitotic division of a D-Mel cell expressing Lamin-GFP and H2A-RFP after transfection with the KAN dsRNA (control). Z-projection of 3 planes of focus through the nucleus. Scale bars: 10 μm.
(AVI)

S2 Movie. Abnormal mitotic division of a D-Mel cell expressing Lamin-GFP and H2A-RFP after transfection with dsRNA against CycB3. Anaphase is delayed and chromosome segregation is defective. Z-projection of 3 planes of focus through the nucleus. Scale bars: 10 μm.
(AVI)

S3 Movie. CycB is rapidly degraded before anaphase onset in a D-Mel cell. Normal mitosis in a D-Mel cell expressing CycB-GFP and Lamin-RFP transfected with KAN dsRNA (control). CycB-GFP localizes on the spindle, kinetochores and centrosomes during mitosis. Z-projection of 3 planes of focus through the nucleus. Scale bars: 10 μm.
(AVI)

S4 Movie. CycB degradation is slower and anaphase is delayed in a dividing D-Mel cell depleted of CycB3. Cell expressing CycB-GFP and Lamin-RFP and transfected with CycB3 dsRNA. Z-projection of 2 planes of focus through the nucleus. Scale bars: 10 μm.
(AVI)

S5 Movie. CycB degradation is incomplete in a D-Mel cell depleted of CycB3 undergoing cytokinesis without anaphase. Cell expressing CycB-GFP and Lamin-RFP and transfected with CycB3 dsRNA. CycB-GFP persists on the chromosomes and centrosomes during cytokinesis. Z-projection of 3 planes of focus through the nucleus. Scale bars: 10 μm.
(AVI)

S6 Movie. CycB3 localization dynamics in a dividing D-Mel cell. CycB3-GFP localizes to chromosomes and spindle poles in early mitosis. Z-projection of 3 planes of focus through the nucleus. Scale bars: 10 μm.
(AVI)

S7 Movie. APC/C localization dynamics in a syncytial embryo. GFP-APC3 becomes enriched in nuclei during mitotic entry and localizes near chromosomes (marked with H2A-RFP) during mitosis. GFP-APC3 also strongly localizes to nuclear envelopes.
(AVI)

S8 Movie. Relative localizations of CycB3 and the APC/C in a dividing D-Mel cell. CycB3-GFP and APC3-RFP both localize to chromosomes before anaphase. Z-projection of 3 planes of focus through the nucleus. Scale bars: 10 μm.
(AVI)

S1 Fig Numerical Data.
(XLSX)

S2 Fig Numerical Data.
(XLSX)

S3 Fig Numerical Data.
(XLSX)

S4 Fig Numerical Data.
(XLSX)

S5 Fig Numerical Data.
(XLSX)

S6 Fig Numerical Data.
(XLSX)

Acknowledgments

We thank Myreille Larouche for making Fig 5, and David Kachaner and other members of the Archambault lab for useful discussions. We are grateful to Christian Charbonneau for help with the microscopy. We thank Christian Lehner for a gift of anti-Cyclin B3 antibody, and Yuu Kimata for pUb-GFP-APC3 and pUb-GFP-APC6 flies.

Author Contributions

Conceptualization: Damien Garrido, Mohammed Bourouh, Éric Bonneil, Pierre Thibault, Andrew Swan, Vincent Archambault.

Formal analysis: Damien Garrido, Mohammed Bourouh, Éric Bonneil, Vincent Archambault.

Funding acquisition: Damien Garrido, Andrew Swan, Vincent Archambault.

Investigation: Damien Garrido, Mohammed Bourouh, Éric Bonneil, Andrew Swan, Vincent Archambault.

Methodology: Damien Garrido, Mohammed Bourouh, Éric Bonneil, Pierre Thibault, Vincent Archambault.

Project administration: Andrew Swan, Vincent Archambault.

Resources: Pierre Thibault, Andrew Swan, Vincent Archambault.

Supervision: Pierre Thibault, Andrew Swan, Vincent Archambault.

Writing – original draft: Damien Garrido, Mohammed Bourouh, Éric Bonneil, Pierre Thibault, Andrew Swan, Vincent Archambault.

References

1. Morgan DO. The Cell Cycle: Principles of Control. London: New Science Press; 2007. 297 p.
2. Holder J, Poser E, Barr FA. Getting out of mitosis: spatial and temporal control of mitotic exit and cytokinesis by PP1 and PP2A. FEBS Lett. 2019; 593(20):2908–24. https://doi.org/10.1002/1873-3468.13595 PMID: 31494926
3. Schellhaus AK, De Magistris P, Antonin W. Nuclear Reformation at the End of Mitosis. J Mol Biol. 2016; 428(10 Pt A):1962–85. https://doi.org/10.1016/j.jmb.2015.09.016 PMID: 26423234
4. Yamano H. APC/C: current understanding and future perspectives. F1000Res. 2019; 8. https://doi.org/10.12688/f1000research.18582.1 PMID: 31164978

5. Alfieri C, Zhang S, Barford D. Visualizing the complex functions and mechanisms of the anaphase promoting complex/cyclosome (APC/C). Open Biol. 2017; 7(11).
6. King RW, Peters JM, Tugendreich S, Rolfe M, Hieter P, Kirschner MW. A 20S complex containing CDC27 and CDC16 catalyzes the mitosis-specific conjugation of ubiquitin to cyclin B. Cell. 1995; 81(2):279–88. https://doi.org/10.1016/0092-8674(95)90338-0 PMID: 7736580
7. Sudakin V, Ganoth D, Dahan A, Heller H, Hershko J, Luca FC, et al. The cyclosome, a large complex containing cyclin-selective ubiquitin ligase activity, targets cyclins for destruction at the end of mitosis. Mol Biol Cell. 1995; 6(2):185–97. https://doi.org/10.1091/mbc.6.2.185 PMID: 7787245
8. Funabiki H, Yamano H, Kumada K, Nagao K, Hunt T, Yanagida M. Cut2 proteolysis required for sister-chromatid seperation in fission yeast. Nature. 1996; 381(6581):438–41. https://doi.org/10.1038/381438a0 PMID: 8632802
9. Cohen-Fix O, Peters JM, Kirschner MW, Koshland D. Anaphase initiation in Saccharomyces cerevisiae is controlled by the APC-dependent degradation of the anaphase inhibitor Pds1p. Genes Dev. 1996; 10(24):3081–93. https://doi.org/10.1101/gad.10.24.3081 PMID: 8985178
10. Ciosk R, Zachariae W, Michaelis C, Shevchenko A, Mann M, Nasmyth K. An ESP1/PDS1 complex regulates loss of sister chromatid cohesion at the metaphase to anaphase transition in yeast. Cell. 1998; 93(6):1067–76. https://doi.org/10.1016/s0092-8674(00)81211-8 PMID: 9635435
11. Uhlmann F, Lottspeich F, Nasmyth K. Sister-chromatid separation at anaphase onset is promoted by cleavage of the cohesin subunit Scc1. Nature. 1999; 400(6739):37–42. https://doi.org/10.1038/21831 PMID: 10403247
12. Visintin R, Prinz S, Amon A. CDC20 and CDH1: a family of substrate-specific activators of APC-dependent proteolysis. Science. 1997; 278(5337):460–3. https://doi.org/10.1126/science.278.5337.460 PMID: 9334304
13. Fang G, Yu H, Kirschner MW. Direct binding of CDC20 protein family members activates the anaphase-promoting complex in mitosis and G1. Mol Cell. 1998; 2(2):163–71. https://doi.org/10.1016/s1097-2765(00)80126-4 PMID: 9734353
14. Corbett KD. Molecular Mechanisms of Spindle Assembly Checkpoint Activation and Silencing. Prog Mol Subcell Biol. 2017; 56:429–55. https://doi.org/10.1007/978-3-319-58592-5_18 PMID: 28840248
15. Labit H, Fujimitsu K, Bayin NS, Takaki T, Gannon J, Yamano H. Dephosphorylation of Cdc20 is required for its C-box-dependent activation of the APC/C. EMBO J. 2012; 31(15):3351–62. https://doi.org/10.1038/emboj.2012.168 PMID: 22713866
16. Fujimitsu K, Yamano H. PP2A-B56 binds to Apc1 and promotes Cdc20 association with the APC/C ubiquitin ligase in mitosis. EMBO Rep. 2020; 21(1):e48503. https://doi.org/10.15252/embr.201948503 PMID: 31825153
17. Hein JB, Hertz EPT, Garvanska DH, Kruse T, Nilsson J. Distinct kinetics of serine and threonine dephosphorylation are essential for mitosis. Nat Cell Biol. 2017; 19(12):1433–40. https://doi.org/10.1038/ncb3634 PMID: 29084198
18. Kramer ER, Scheuringer N, Podtelejnikov AV, Mann M, Peters JM. Mitotic regulation of the APC activator proteins CDC20 and CDH1. Mol Biol Cell. 2000; 11(5):1555–69. https://doi.org/10.1091/mbc.11.5.1555 PMID: 10793135
19. Zhang S, Chang L, Alfieri C, Zhang Z, Yang J, Maslen S, et al. Molecular mechanism of APC/C activation by mitotic phosphorylation. Nature. 2016; 533(7602):260–4. https://doi.org/10.1038/nature17973 PMID: 27120157
20. Fujimitsu K, Grimaldi M, Yamano H. Cyclin-dependent kinase 1-dependent activation of APC/C ubiquitin ligase. Science. 2016; 352(6289):1121–4. https://doi.org/10.1126/science.aad3925 PMID: 27103671
21. Fung TK, Poon RY. A roller coaster ride with the mitotic cyclins. Semin Cell Dev Biol. 2005; 16(3):335–42. https://doi.org/10.1016/j.semcdb.2005.02.014 PMID: 15840442
22. Li J, Qian WP, Sun QY. Cyclins regulating oocyte meiotic cell cycle progressiondagger. Biol Reprod. 2019; 101(5):878–81. https://doi.org/10.1093/biolre/ioz143 PMID: 31347666
23. Hein JB, Nilsson J. Interphase APC/C-Cdc20 inhibition by cyclin A2-Cdk2 ensures efficient mitotic entry. Nat Commun. 2016; 7:10975. https://doi.org/10.1038/ncomms10975 PMID: 26960431
24. Lindqvist A, Rodriguez-Bravo V, Medema RH. The decision to enter mitosis: feedback and redundancy in the mitotic entry network. J Cell Biol. 2009; 185(2):193–202. https://doi.org/10.1083/jcb.200812045 PMID: 19364923
25. Zhang Y, Zhu CC, Sun SC. Cyclin B3: an anaphase onset controller in meiosis. Cell Cycle. 2015; 14(19):3013. https://doi.org/10.1080/15384101.2015.1084201 PMID: 26496167
26. Gallant P, Nigg EA. Identification of a novel vertebrate cyclin: cyclin B3 shares properties with both A- and B-type cyclins. EMBO J. 1994; 13(3):595–605. PMID: 8313904

27. McCleland ML, Farrell JA, O'Farrell PH. Influence of cyclin type and dose on mitotic entry and progression in the early Drosophila embryo. J Cell Biol. 2009; 184(5):639–46. https://doi.org/10.1083/jcb.200810012 PMID: 19273612

28. Yuan K, O'Farrell PH. Cyclin B3 is a mitotic cyclin that promotes the metaphase-anaphase transition. Curr Biol. 2015; 25(6):811–6. https://doi.org/10.1016/j.cub.2015.01.053 PMID: 25754637

29. Lehner CF, O'Farrell PH. Expression and function of Drosophila cyclin A during embryonic cell cycle progression. Cell. 1989; 56(6):957–68. https://doi.org/10.1016/0092-8674(89)90629-6 PMID: 2564316

30. Reber A, Lehner CF, Jacobs HW. Terminal mitoses require negative regulation of Fzr/Cdh1 by Cyclin A, preventing premature degradation of mitotic cyclins and String/Cdc25. Development. 2006; 133 (16):3201–11. https://doi.org/10.1242/dev.02488 PMID: 16854973

31. Jacobs HW, Knoblich JA, Lehner CF. Drosophila Cyclin B3 is required for female fertility and is dispensable for mitosis like Cyclin B. Genes Dev. 1998; 12(23):3741–51. https://doi.org/10.1101/gad.12.23.3741 PMID: 9851980

32. Bourouh M, Dhaliwal R, Rana K, Sinha S, Guo Z, Swan A. Distinct and Overlapping Requirements for Cyclins A, B, and B3 in Drosophila Female Meiosis. G3 (Bethesda). 2016; 6(11):3711–24.

33. Zhang T, Qi ST, Huang L, Ma XS, Ouyang YC, Hou Y, et al. Cyclin B3 controls anaphase onset independent of spindle assembly checkpoint in meiotic oocytes. Cell Cycle. 2015; 14(16):2648–54. https://doi.org/10.1080/15384101.2015.1064567 PMID: 26125114

34. Karasu ME, Bouftas N, Keeney S, Wassmann K. Cyclin B3 promotes anaphase I onset in oocyte meiosis. J Cell Biol. 2019; 218(4):1265–81. https://doi.org/10.1083/jcb.201808091 PMID: 30723090

35. Li Y, Wang L, Zhang L, He Z, Feng G, Sun H, et al. Cyclin B3 is required for metaphase to anaphase transition in oocyte meiosis I. J Cell Biol. 2019; 218(5):1553–63. https://doi.org/10.1083/jcb.201808088 PMID: 30770433

36. Deyter GM, Furuta T, Kurasawa Y, Schumacher JM. Caenorhabditis elegans cyclin B3 is required for multiple mitotic processes including alleviation of a spindle checkpoint-dependent block in anaphase chromosome segregation. PLoS Genet. 2010; 6(11):e1001218. https://doi.org/10.1371/journal.pgen.1001218 PMID: 21124864

37. Mehsen H, Boudreau V, Garrido D, Bourouh M, Larouche M, Maddox PS, et al. PP2A-B55 promotes nuclear envelope reformation after mitosis in Drosophila. J Cell Biol. 2018; 217(12):4106–23. https://doi.org/10.1083/jcb.201804018 PMID: 30309980

38. Mayer-Jaekel RE, Ohkura H, Ferrigno P, Andjelkovic N, Shiomi K, Uemura T, et al. Drosophila mutants in the 55 kDa regulatory subunit of protein phosphatase 2A show strongly reduced ability to dephosphorylate substrates of p34cdc2. J Cell Sci. 1994; 107 (Pt 9):2609–16. PMID: 7844174

39. Li D, Morley G, Whitaker M, Huang JY. Recruitment of Cdc20 to the kinetochore requires BubR1 but not Mad2 in Drosophila melanogaster. Mol Cell Biol. 2010; 30(13):3384–95. https://doi.org/10.1128/MCB.00258-10 PMID: 20421417

40. Swan A, Schupbach T. The Cdc20 (Fzy)/Cdh1-related protein, Cort, cooperates with Fzy in cyclin destruction and anaphase progression in meiosis I and II in Drosophila. Development. 2007; 134 (5):891–9. https://doi.org/10.1242/dev.02784 PMID: 17251266

41. Dawson IA, Roth S, Artavanis-Tsakonas S. The Drosophila cell cycle gene fizzy is required for normal degradation of cyclins A and B during mitosis and has homology to the CDC20 gene of Saccharomyces cerevisiae. J Cell Biol. 1995; 129(3):725–37. https://doi.org/10.1083/jcb.129.3.725 PMID: 7730407

42. Pesin JA, Orr-Weaver TL. Developmental role and regulation of cortex, a meiosis-specific anaphase-promoting complex/cyclosome activator. PLoS Genet. 2007; 3(11):e202. https://doi.org/10.1371/journal.pgen.0030202 PMID: 18020708

43. Knoblich JA, Lehner CF. Synergistic action of Drosophila cyclins A and B during the G2-M transition. EMBO J. 1993; 12(1):65–74. PMID: 8428595

44. Wang Z, Lin H. The division of Drosophila germline stem cells and their precursors requires a specific cyclin. Curr Biol. 2005; 15(4):328–33. https://doi.org/10.1016/j.cub.2005.02.016 PMID: 15723793

45. Echard A, O'Farrell PH. The degradation of two mitotic cyclins contributes to the timing of cytokinesis. Curr Biol. 2003; 13(5):373–83. https://doi.org/10.1016/s0960-9822(03)00127-1 PMID: 12620185

46. Huang JY, Raff JW. The dynamic localisation of the Drosophila APC/C: evidence for the existence of multiple complexes that perform distinct functions and are differentially localised. J Cell Sci. 2002; 115 (Pt 14):2847–56. PMID: 12082146

47. Hegemann B, Hutchins JR, Hudecz O, Novatchkova M, Rameseder J, Sykora MM, et al. Systematic phosphorylation analysis of human mitotic protein complexes. Sci Signal. 2011; 4(198):rs12. https://doi.org/10.1126/scisignal.2001993 PMID: 22067460

48. Sigrist S, Jacobs H, Stratmann R, Lehner CF. Exit from mitosis is regulated by Drosophila fizzy and the sequential destruction of cyclins A, B and B3. EMBO J. 1995; 14(19):4827–38. PMID: 7588612

49. Raff JW, Jeffers K, Huang JY. The roles of Fzy/Cdc20 and Fzr/Cdh1 in regulating the destruction of cyclin B in space and time. J Cell Biol. 2002; 157(7):1139–49. https://doi.org/10.1083/jcb.200203035 PMID: 12082076

50. Patra D, Dunphy WG. Xe-p9, a Xenopus Suc1/Cks protein, is essential for the Cdc2-dependent phosphorylation of the anaphase- promoting complex at mitosis. Genes Dev. 1998; 12(16):2549–59. https://doi.org/10.1101/gad.12.16.2549 PMID: 9716407

51. Shteinberg M, Hershko A. Role of Suc1 in the activation of the cyclosome by protein kinase Cdk1/cyclin B. Biochem Biophys Res Commun. 1999; 257(1):12–8. https://doi.org/10.1006/bbrc.1999.0409 PMID: 10092502

52. Bourne Y, Watson MH, Hickey MJ, Holmes W, Rocque W, Reed SI, et al. Crystal structure and mutational analysis of the human CDK2 kinase complex with cell cycle-regulatory protein CksHs1. Cell. 1996; 84(6):863–74. https://doi.org/10.1016/s0092-8674(00)81065-x PMID: 8601310

53. Koivomagi M, Valk E, Venta R, Iofik A, Lepiku M, Balog ER, et al. Cascades of multisite phosphorylation control Sic1 destruction at the onset of S phase. Nature. 2011; 480(7375):128–31. https://doi.org/10.1038/nature10560 PMID: 21993622

54. McGrath DA, Balog ER, Koivomagi M, Lucena R, Mai MV, Hirschi A, et al. Cks confers specificity to phosphorylation-dependent CDK signaling pathways. Nat Struct Mol Biol. 2013; 20(12):1407–14. https://doi.org/10.1038/nsmb.2707 PMID: 24186063

55. Huang JY, Morley G, Li D, Whitaker M. Cdk1 phosphorylation sites on Cdc27 are required for correct chromosomal localisation and APC/C function in syncytial Drosophila embryos. J Cell Sci. 2007; 120(Pt 12):1990–7. https://doi.org/10.1242/jcs.006833 PMID: 17519285

56. Parry DH, O'Farrell PH. The schedule of destruction of three mitotic cyclins can dictate the timing of events during exit from mitosis. Curr Biol. 2001; 11(9):671–83. https://doi.org/10.1016/s0960-9822(01)00204-4 PMID: 11369230

57. Casas-Vila N, Bluhm A, Sayols S, Dinges N, Dejung M, Altenhein T, et al. The developmental proteome of Drosophila melanogaster. Genome Res. 2017; 27(7):1273–85. https://doi.org/10.1101/gr.213694.116 PMID: 28381612

58. Bloom J, Cross FR. Multiple levels of cyclin specificity in cell-cycle control. Nat Rev Mol Cell Biol. 2007; 8(2):149–60. https://doi.org/10.1038/nrm2105 PMID: 17245415

59. Lara-Gonzalez P, Moyle MW, Budrewicz J, Mendoza-Lopez J, Oegema K, Desai A. The G2-to-M Transition Is Ensured by a Dual Mechanism that Protects Cyclin B from Degradation by Cdc20-Activated APC/C. Dev Cell. 2019; 51(3):313–25 e10. https://doi.org/10.1016/j.devcel.2019.09.005 PMID: 31588029

60. D'Avino PP, Archambault V, Przewloka MR, Zhang W, Laue ED, Glover DM. Isolation of protein complexes involved in mitosis and cytokinesis from Drosophila cultured cells. Methods Mol Biol. 2009; 545:99–112. https://doi.org/10.1007/978-1-60327-993-2_6 PMID: 19475384

61. Dernburg A. In situ hybridization to somatic chromosomes. In: Sullivan W, Ashburner M., Hawley R.S., editor. Drosophila Protocols Cold Spring Harbour: Cold Spring Harbour Laboratory Press.; 2000. p. 25–55.

62. Kachaner D, Garrido D, Mehsen H, Normandin K, Lavoie H, Archambault V. Coupling of Polo kinase activation to nuclear localization by a bifunctional NLS is required during mitotic entry. Nat Commun. 2017; 8(1):1701. https://doi.org/10.1038/s41467-017-01876-8 PMID: 29167465